The Impact of Stratocumulus Cloud Radiative Properties on Surface Heat Fluxes Simulated with a General Circulation Model

JUI-LIN F. LI

Research Data Corporation, Data Assimilation Office, NASA, Greenbelt, Maryland

MARTIN KÖHLER

European Centre for Medium-Range Weather Forecasts, Reading, United Kingdom

JOHN D. FARRARA AND C. R. MECHOSO

Department of Atmospheric Sciences, University of California, Los Angeles, Los Angeles, California

26 February 2001 and 5 November 2001

ABSTRACT

When sea surface temperatures are prescribed at its lower boundary, the University of California, Los Angeles (UCLA) atmospheric general circulation model (AGCM) produces a realistic simulation of planetary boundary layer (PBL) stratocumulus cloud incidence. Despite this success, net surface solar fluxes are generally overpredicted in comparison to Earth Radiation Budget Experiment (ERBE) derived data in regions characterized by persistent stratocumulus cloud decks. It is suggested that this deficiency is due to the highly simplified formulation of the PBL cloud optical properties. A new formulation of PBL cloud optical properties is developed based on an estimate of the stratocumulus cloud liquid water path. The January and July mean net surface solar fluxes simulated by the revised AGCM are closer to ERBE-derived values in regions where stratocumulus clouds are frequently observed. The area-averaged estimated error reductions range from 24 (Peru region) to 53 W m^{-2} (South Pacific storm track region). The results emphasize that surface heat fluxes are very sensitive to the radiative properties of stratocumulus clouds and that a realistic simulation of both the geographical distribution of stratocumulus clouds and their optical properties is crucial.

1. Introduction

Persistent stratocumulus clouds cover a significant portion of the earth's surface and particularly of the world's oceans (Klein and Hartmann 1993). Their importance in the global radiation budget arises from the fact that they reflect more solar energy (~60%) back to space than the underlying ocean surface does (~ less than 10%). The interactive roles of stratocumulus clouds, their radiative properties, and their impacts on the surface energy budget have been studied for several decades following the pioneering observational work of Neiburger et al. (1961) and the modeling studies of Lilly (1968) and Schubert (1976). These authors demonstrated that a stratocumulus cloud deck typically occupies the upper portion of a well-mixed planetary boundary layer (PBL), that turbulence within the cloud layer is primarily generated by radiative cooling at cloud top, and that the clouds have a substantial impact on the surface energy budget.

In view of their importance in the surface energy budget, most atmospheric general circulation models (AGCMs) predict or diagnose PBL stratocumulus cloud amounts and their radiative impacts. However, most AGCMs substantially underestimate PBL cloud amounts (Wyngaard and Moeng 1990), resulting in an overestimate of surface solar radiative fluxes. When an AGCM with such difficulties is coupled to an oceanic model, there are typically large errors in the simulated sea surface temperatures (SSTs) in the regions along the coasts of California and Peru where persistent stratocumulus decks are observed. The correction of such errors is important for a successful simulation with a coupled atmosphere–ocean GCM of the seasonal cycle and interannual variability (the El Niño-Southern Oscillation phenomenon) in tropical Pacific SSTs. There

Corresponding author address: Dr. John D. Farrara, Dept. of Atmospheric Sciences, University of California, Los Angeles, 405 Hilgard Ave., Los Angeles, CA 90095-1565.
E-mail: farrara@atmos.ucla.edu

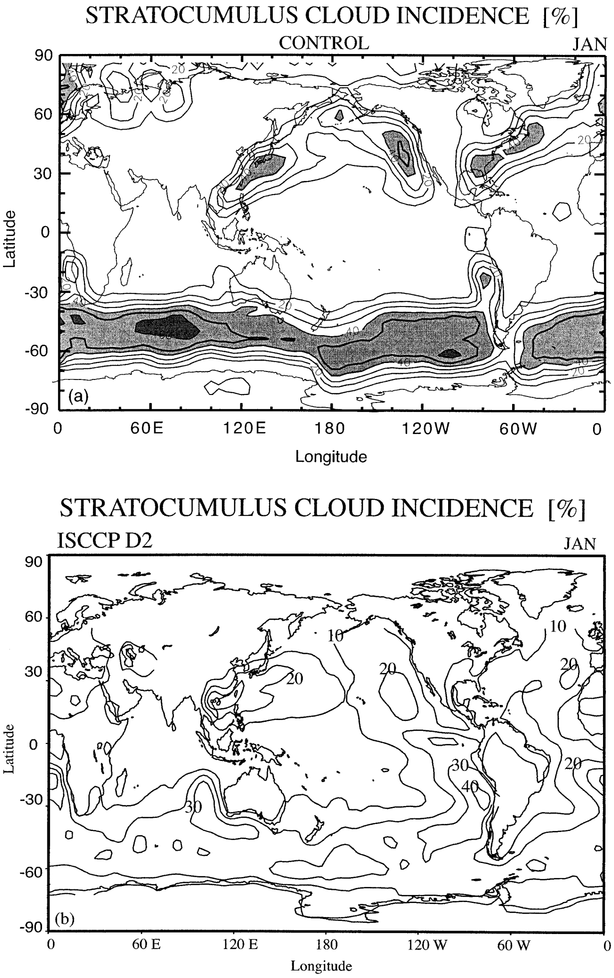

FIG. 1. (a) Simulated Jan mean PBL stratocumulus cloud incidence using the CONTROL version of the UCLA AGCM. The contour interval is 10%. (b) As in (a) but for the 8-yr (1986–93) average Jan monthly mean stratocumulus clouds derived from the ISCCP-D2 dataset.

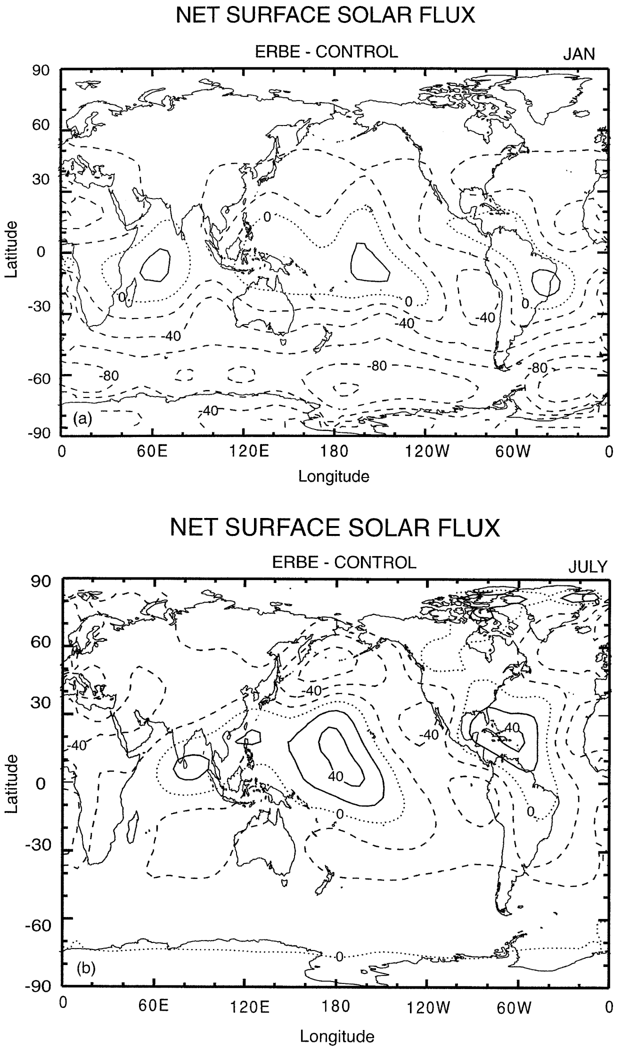

FIG. 2. (a) The difference in Jan mean net surface solar flux between the CONTROL simulation and ERBE observations. (b) As in (a) but for Jul. The zero contour is dotted. The contour interval is 20 W m^{-2}.

are also significant amounts of stratocumulus clouds in mid- and high latitudes. These should also be realistically simulated due to their importance for simulation of anthropogenic climate change.

An earlier version of the University of California, Los Angeles (UCLA), AGCM (with prescribed SSTs) substantially underestimated stratocumulus cloud incidence and when coupled to the Modular Ocean Model (MOM) produced the errors described in the previous paragraph (see Ma et al. 1996; Mechoso et al. 2000). In the UCLA AGCM, the model's vertical coordinate is based on a modified-sigma system in which the lowest layer itself is the PBL and it can be cloud topped (Suarez et al. 1983). With this coordinate, it is easier to explicitly formulate processes at the PBL top. Thus, the AGCM vertical structure is particularly suitable for attempts to alleviate such an underestimate of stratiform cloud amount. Li and Arakawa (1997) carried out an extensive revision of the formulation of the PBL moist processes in the AGCM. The revisions they implemented included 1) a revised formulation of the properties of air entrained into the PBL, 2) a revised formulation of the entrainment process when stratocumulus clouds are unstable, and 3) inclusion of a simple formulation of the subgrid-scale orographic effects on the fractional PBL cloudiness. The model with these modifications produces more realistic simulations of stratocumulus incidence in all seasons (Fig. 1a shows the simulated incidence for January) compared to the observations of Klein and Hartmann (1993) and the International Satellite Cloud Climatology Project (ISCCP-D2) dataset (Fig. 1b shows ISCCP-D2 January low cloud incidence). The same version, coupled to a tropical Pacific version of MOM, showed dramatic improvements in the simulated annual cycle, interannual variability, and annual mean of the tropical SST (Mechoso et al. 2000).

The improvement in the simulation of PBL stratocu-

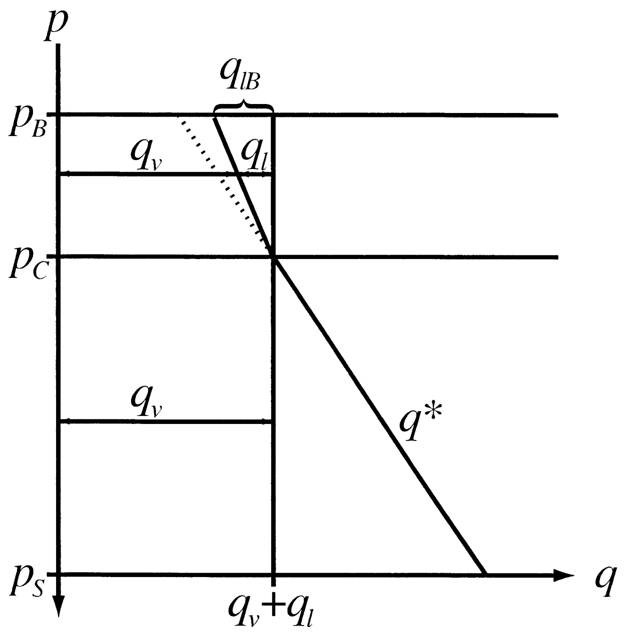

FIG. 3. The vertical structure of the total water mixing ratio $r_M = q_v + q_l$ and water vapor mixing ratio q_v in a cloud-topped PBL. Here, p_C is the pressure at the condensation level; p_S and p_B are the surface and PBL top pressures, and q^* is the saturation value of water vapor mixing ratio.

mulus cloud incidence, however, did not have a counterpart in the net solar and total heat fluxes at the surface. Figure 2a, for example, shows that the AGCM overestimates, by up to 80–100 W m^{-2}, the net surface solar fluxes over the low pressure belt around Antarctica during the southern summer in reference to values derived from the Earth Radiation Budget Experiment (ERBE) dataset (Li and Leighton 1993, Fig. 2a). There is a similar overestimation of up to 40–60 W m^{-2} over the North Pacific Ocean during the northern summer (Fig. 2b). Here, simulated SSTs are too warm when the AGCM is coupled to an oceanic GCM (OGCM) (J. Farrara 1998, unpublished manuscript). The overestimation of net solar fluxes is consistent with smaller stratocumulus cloud optical thicknesses than those estimated using ISCCP-D2 data (see Figs. 4e and 4f; Rossow et al. 1996).

In the model that produced Fig. 2, stratocumulus cloud optical thickness is simply proportional to cloud depth. It has been recognized, however, that cloud properties such as the vertical integral of liquid water path (LWP) and the cloud particle size distribution can have large impacts on PBL cloud radiative properties (Gultepe and Isaac 1997). In most AGCMs, the determination of LWP in PBL stratiform clouds is based either on an empirical relative humidity diagnosis, as in Sundqvist (1978), or on a prognostic cloud liquid water formulation, as in Del Genio et al. (1996), with no distinction between PBL and free-atmosphere clouds (Wyngaard and Moeng 1990). In the UCLA AGCM (Suarez et al. 1983), the stratocumulus-topped PBL is explicitly formulated and a diagnostic estimate of PBL cloud LWP can be made.

This note describes the sensitivity of surface fluxes simulated by the AGCM to simple specifications of PBL cloud radiative properties. We ask whether significant improvement can be obtained without major model upgrades in the radiation parameterization or the incorporation of expensive calculations such as those needed by microphysical processes. In particular, we examine the impact of including a simple formulation of LWP in the calculation of stratocumulus cloud optical thickness.

Section 2 of the paper describes the revision of PBL cloud radiative properties that was made along the lines described in the previous paragraphs. Section 3 presents comparisons of simulations with and without the revision. Section 4 discusses our findings.

2. Stratocumulus cloud radiative properties

a. Model description

The UCLA AGCM is a finite-difference model based on the primitive equations, with horizontal velocity, potential temperature, surface pressure, water vapor mixing ratio, ground temperature, and snow depth over land as the model's prognostic variables. Solar and terrestrial radiation, as well as cloud radiative properties, are parameterized following Harshvardhan et al. (1989). This parameterization considers two types of clouds: 1) cumulus anvil clouds associated with subgrid-scale convection which are assumed to occur only above 500 hPa, and 2) layer clouds associated with grid-scale supersaturation, which include PBL stratocumulus. For both types of clouds, cloud emissivities depend on pressure thickness of the layer and temperature in a functional form that has different coefficients for cumulus and layer clouds. These differences are such that, for clouds of the same pressure thickness and temperature, cumulus anvil clouds have a somewhat larger emissivity than layer clouds. In this study we use a version of the model that has 15 layers in the vertical, with the model top at 1 mb, and a horizontal resolution of 5° in latitude and 4° in longitude. More details of the model are given in Mechoso et al. (2000) and references therein. All results presented here were obtained in 5-yr-long simulations, which use monthly climatological SSTs and start from initial conditions corresponding to 1 October 1982.

b. PBL cloud optical properties

In the PBL parameterization, the stratocumulus cloud condensation level, p_c, is defined as the level at which $q^* = r_M$. Here $q^*(T, p)$ is the saturation value of water vapor mixing ratio and $r_M = q_v + q_l$, where q_v and q_l represent the mixing ratio of water vapor and liquid water, respectively (Suarez et al. 1983). The vertical profile of the saturated water vapor mixing ratio is approximated as linear in pressure (see Fig. 3). The vertical

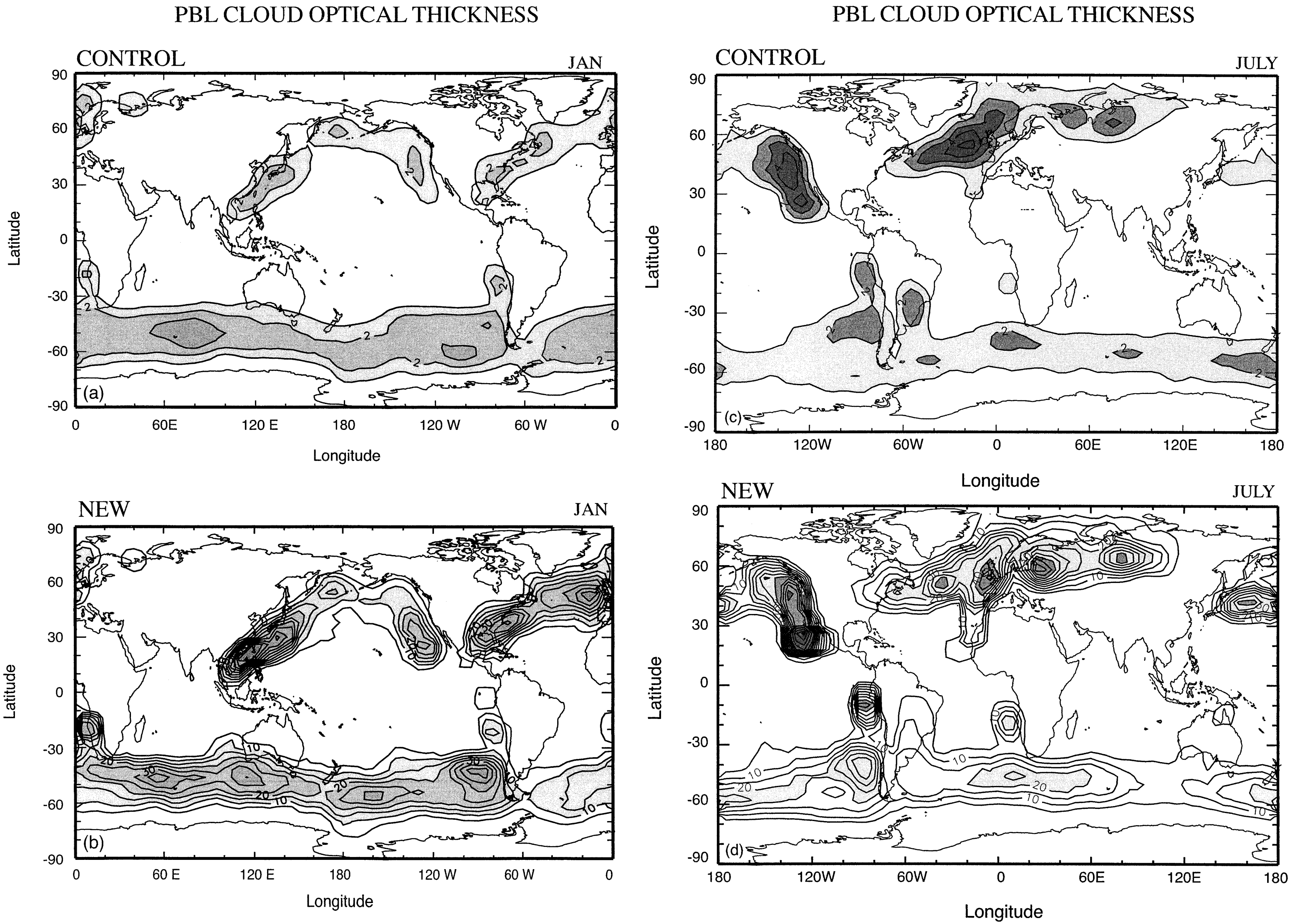

FIG. 4. (a) Simulated Jan mean stratocumulus cloud optical thickness using the CONTROL version. The contour interval is 1. (b) As in (a) but for the NEW version. The contour interval is 5. (c) As in (a) but for Jul. (d) As in (c) but for the NEW version. (e) As in (a) but for 8-yr (1983–96) average Jan monthly mean stratocumulus clouds (liquid only) derived from ISCCP D2 data. (f) As in (e) but for Jul.

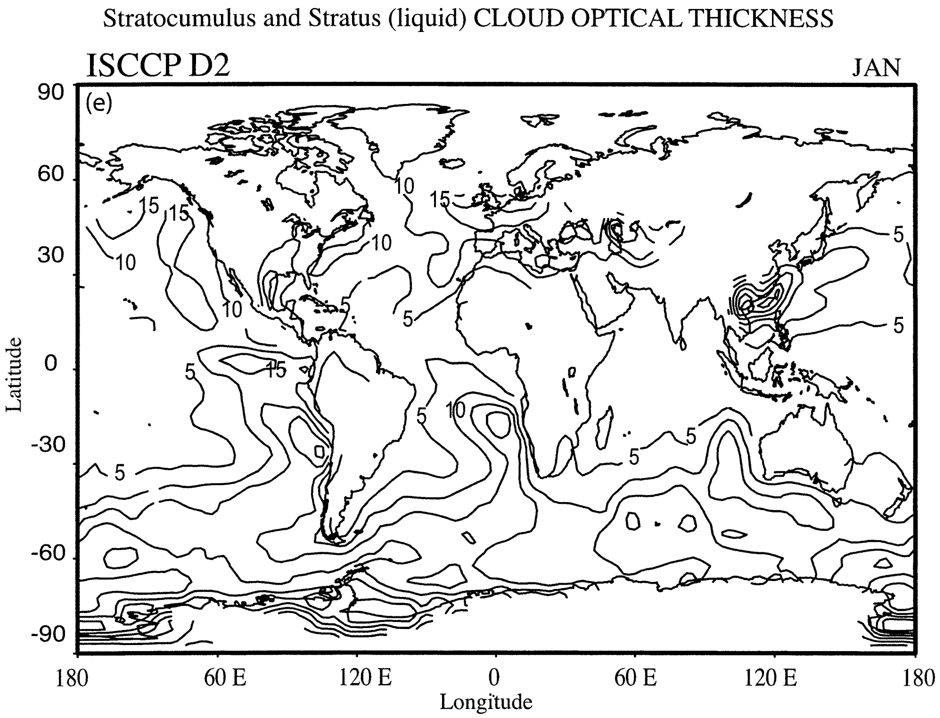

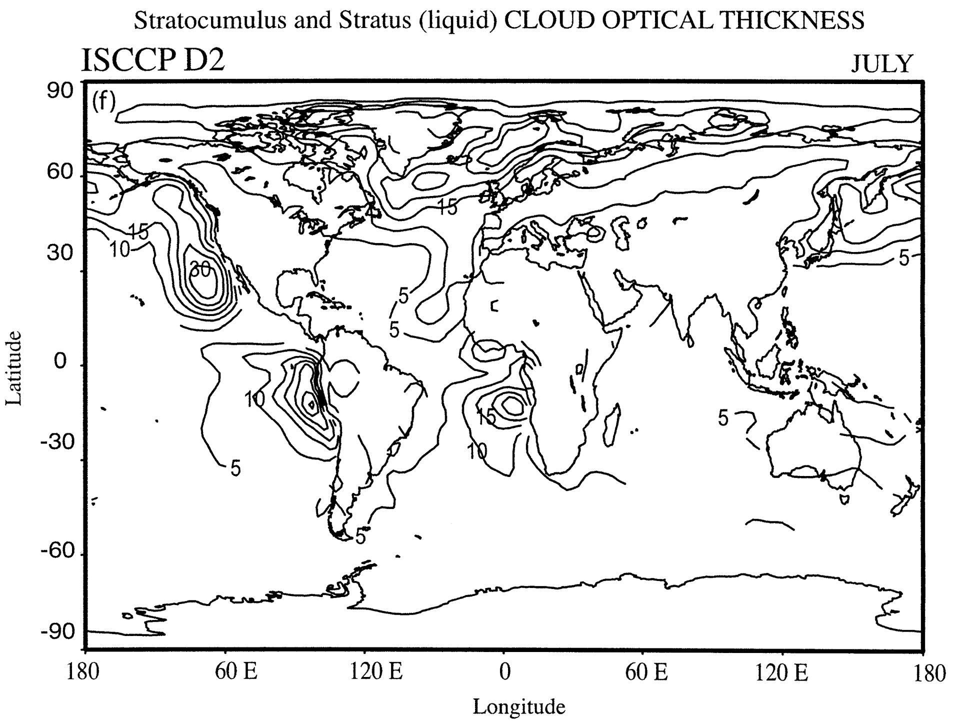

FIG. 4. (*Continued*)

profiles of q_v and q_l are then completely defined by the condensation level and the liquid water mixing ratio at cloud top, q_{lB}. In the PBL, precipitation is assumed to occur only when p_c is greater than the pressure at the earth's surface. By sequestering all condensed water vapor in the cloud, this assumption may lead to an overestimate of the PBL cloud liquid water path (see below), at some times in some regions.

An estimation of cloud radiative fluxes requires the specification of cloud optical thickness. The old formulation following Harshvardhan et al. (1989) determines the solar optical thickness of stratiform clouds according to

$$\tau_{Sc} = \frac{\Delta p_{Sc}}{\alpha}, \quad (1)$$

where Δp_{Sc} ($=p_C - p_B$) represents the cloud pressure thickness and $\alpha = 12.5$ hPa. In addition, a cloud fraction of 1 for values of $\tau_{Sc} > 1$ and a cloud fraction equal to τ_{Sc} for values of $\tau_{Sc} < 1$ are assumed. This formulation produces rather small values of cloud optical thickness when compared to those in the ISCCP-D2 dataset obtained from satellite observations (which are on the order of 3 to 30; see Figs. 4e,f). Using Eq. (1), a cloud with pressure thickness of 30 hPa—a typical value for PBL clouds in our AGCM simulations—has an optical thickness $\tau_{Sc} = 2.4$.

Here, we propose an alternative to (1) following Stephens (1978). He assumed spherical cloud particles with an efficiency factor of 2, which allows the optical thickness to be represented as

$$\tau_{Sc} = \frac{3}{2}\frac{LWP}{\rho_l r_e}, \quad (2)$$

where LWP is the liquid water path, r_e is the effective radius of cloud droplets, and ρ_l is the density of liquid water. For the effective radius of cloud droplets, the global Advanced Very High Resolution Radiometer (AVHRR) satellite data archive indicates an annual mean of 11.4 ± 5.6 μm (Han et al. 1994). The observed variance in cloud droplet size is associated with variations in cloud condensation nuclei (CCN) concentration and liquid water content (LWC) (Han et al. 1994). The extent to which variations in each cause the rather large variance of the annual mean value of r_e is still a subject of debate due to uncertainties in estimates of CCN and LWC. Here, we use a fixed value of 10 μm for r_e.

From the assumptions of a mixed layer PBL and a linear relationship between q_{lB} and pressure, one obtains

$$LWP = \frac{1}{2}q_{lB}\frac{\Delta p_{Sc}}{g}, \quad (3)$$

where g is gravity (D. A. Randall 1994, personal communication). Note, the methodology leading to this value for LWP is consistent with the formulation of the PBL moist processes in the AGCM (Suarez et al. 1983). Finally, using (2) and (3) we obtain

$$\tau_{Sc} = \frac{3}{4}\frac{q_{lB}\Delta p_{Sc}}{\rho_l r_e g}. \quad (4)$$

For a stratocumulus cloud with a pressure thickness of 30 hPa and $q_{lB} = 10^{-3}$ (kg kg^{-1})—values typical of those found in our AGCM simulations—Eq. (4) yields an optical thickness of 23, which is nearly an order of magnitude larger than that given by (1).

The following section of this note presents the results of simulations using either Eq. (1) or (4). These simulations are referred to hereafter as CONTROL and NEW, respectively.

3. The impact of the revision on net surface solar radiative fluxes

The map of January mean stratocumulus cloud incidence obtained with the NEW version is very similar to the distribution simulated in the CONTROL version (see Fig. 1a). Thus, the locations of the maxima off the west coasts of North America, South America, and South Africa, as well as those over the northeastern Atlantic Ocean and the low pressure belt around the Antarctica, are fairly realistically simulated compared to the observations of ISCCP-D2 dataset (see Fig. 1b) and the results of Klein and Hartmann (1993). The corresponding stratocumulus cloud optical depths (Fig. 4b) can be larger than 30 and are typically 5–10 times larger than those in CONTROL (Fig. 4a). The average cloud pressure thickness, however, is almost the same in the two model versions (NEW = 29.9 hPa, CONTROL = 31.8 hPa). In NEW the simulated cloud incidence also slightly decreases, indicating a weak negative feedback of the new radiative properties on cloud formation. Higher cloud optical depths in NEW compared to CONTROL lead to more solar warming in clouds. Two negative feedbacks result: 1) solar heating at the PBL top stabilizes the PBL, decreases the PBL height, and therefore the mixed layer cloud water, and 2) solar heating warms the PBL, reducing cloud water. The effect of the new radiative properties in NEW on the longwave radiation (which drives in-cloud turbulent entrainment in the PBL) is negligible as the emissivities of the clouds are already nearly 1, even in CONTROL.

The magnitude of the optical depths simulated with the NEW version of the model are comparable to that in the ISCCP-D2 low-level stratus and stratocumulus clouds (Rossow et al. 1996). Stratocumulus cloud optical depths are also 5–10 times larger in NEW than in CONTROL both during January (see Figs. 4a and 4b) and July (see Figs. 4c and 4d), and are comparable to that in the 8-yr average of ISCCP-D2 optical depth for stratocumulus and stratus clouds (Fig. 4e for January and Fig. 4f for July). The locations of the simulated maxima are comparable to the ISCCP-D2 dataset off the west coasts of North America, South America, South Africa, and over the northeastern Atlantic Ocean in both January and July, as well as the low pressure belt around

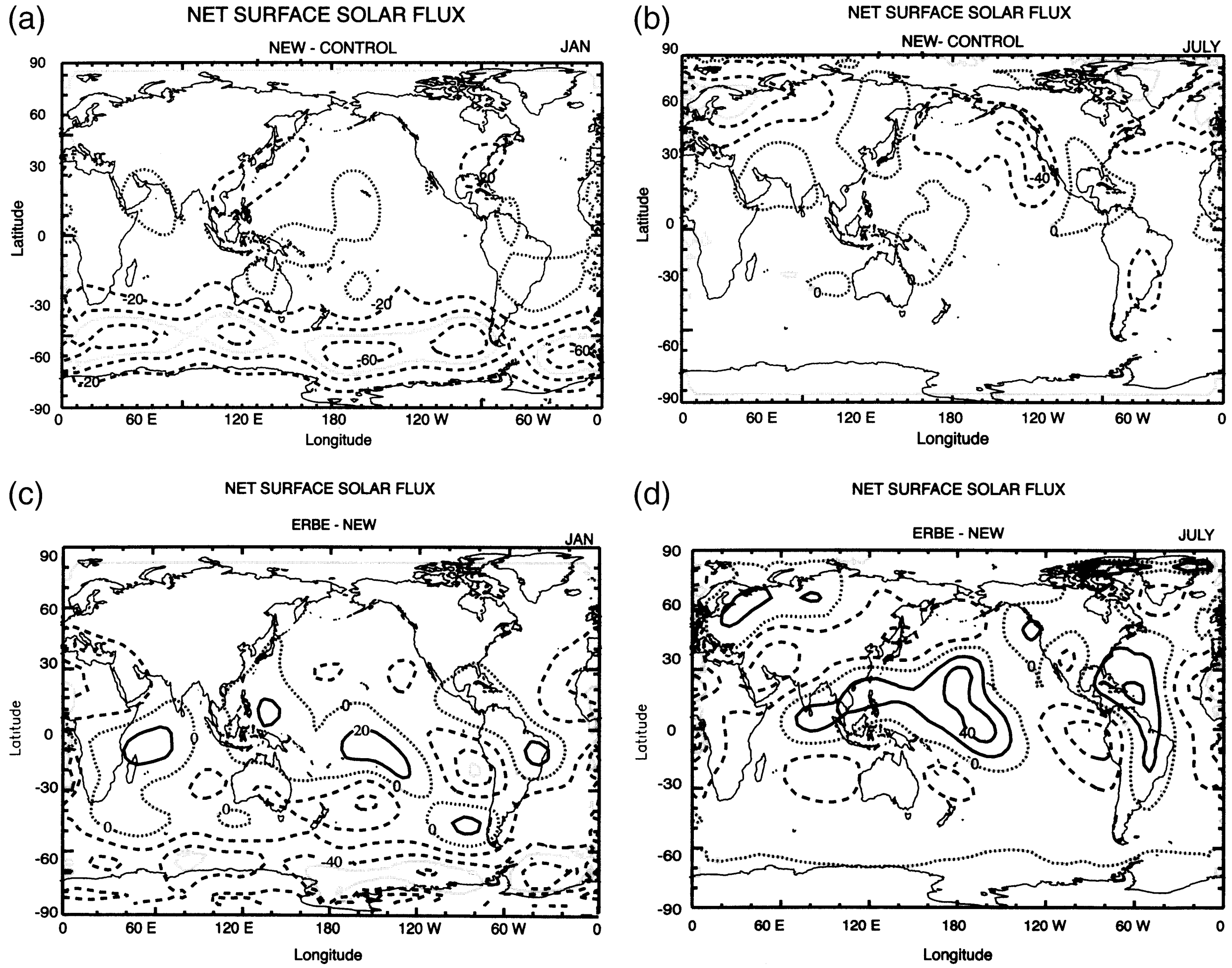

FIG. 5. (a) The difference in Jan mean net surface solar flux between the CONTROL and NEW simulations. (b) As in (a) but for Jul. (c) As in (a) but for the difference between ERBE-derived results and NEW. (d) As in (c) but for Jul. The contour interval is 20 W m^{-2} and the zero contour is dotted.

the Antarctica in January. We note that the ISCCP-D2 cloud optical depths seem to be unrealistically low in July in the low pressure belt around Antarctica. Consistently, simulated net surface solar fluxes are about 40–60 W m^{-2} less than in CONTROL over the low pressure belt around Antarctica in January (Fig. 5a) and about 20–40 W m^{-2} less over the North Pacific and Atlantic Oceans in July (Fig. 5b). In the regions of maximum stratocumulus cloud incidence off the west coasts of South America and South Africa, the differences are more subtle, with net surface solar fluxes in January generally showing reductions of 5–15 W m^{-2}.

In all cases, net surface solar fluxes in NEW are more realistic than those in CONTROL, when compared to those in the ERBE-derived dataset (Li and Leighton 1993). This is clear over the low pressure belt around Antarctica in January (Fig. 5c) and over the North Pacific and the northeastern Atlantic Ocean in July (Fig. 5d). The values of net surface solar fluxes in NEW have positive biases when compared to ERBE-derived values of about 20–40 W m^{-2} (compared to 80–100 W m^{-2} in CONTROL) over the low pressure belt around Antarctica in January (cf. Figs. 2a and 5c) and 5–15 W m^{-2} (compared to 40–60 W m^{-2} in CONTROL) over the North Pacific and northeastern Atlantic Ocean in July (cf. Figs. 2b and 5d).

Figure 6 compares the monthly mean simulated (NEW and CONTROL) and observed net fluxes of latent, solar, terrestrial, and total heat at the surface in four regions during periods when solar radiation is at a maximum: off the coast of California in July (region A), off the coast of Peru in November (region B), around the Antarctic low pressure belt in January (region C), and over the North Atlantic Ocean in July (region D). Here, observed values are taken from the National Centers for Environmental Prediction (NCEP) reanalysis (averaging period: 1968–96) for the net surface heat (NHF), latent (LH), terrestrial (TF) and solar fluxes (SF) of ERBE (averaging period: 1985–89). Several features of this comparison are worthy of discussion. For all

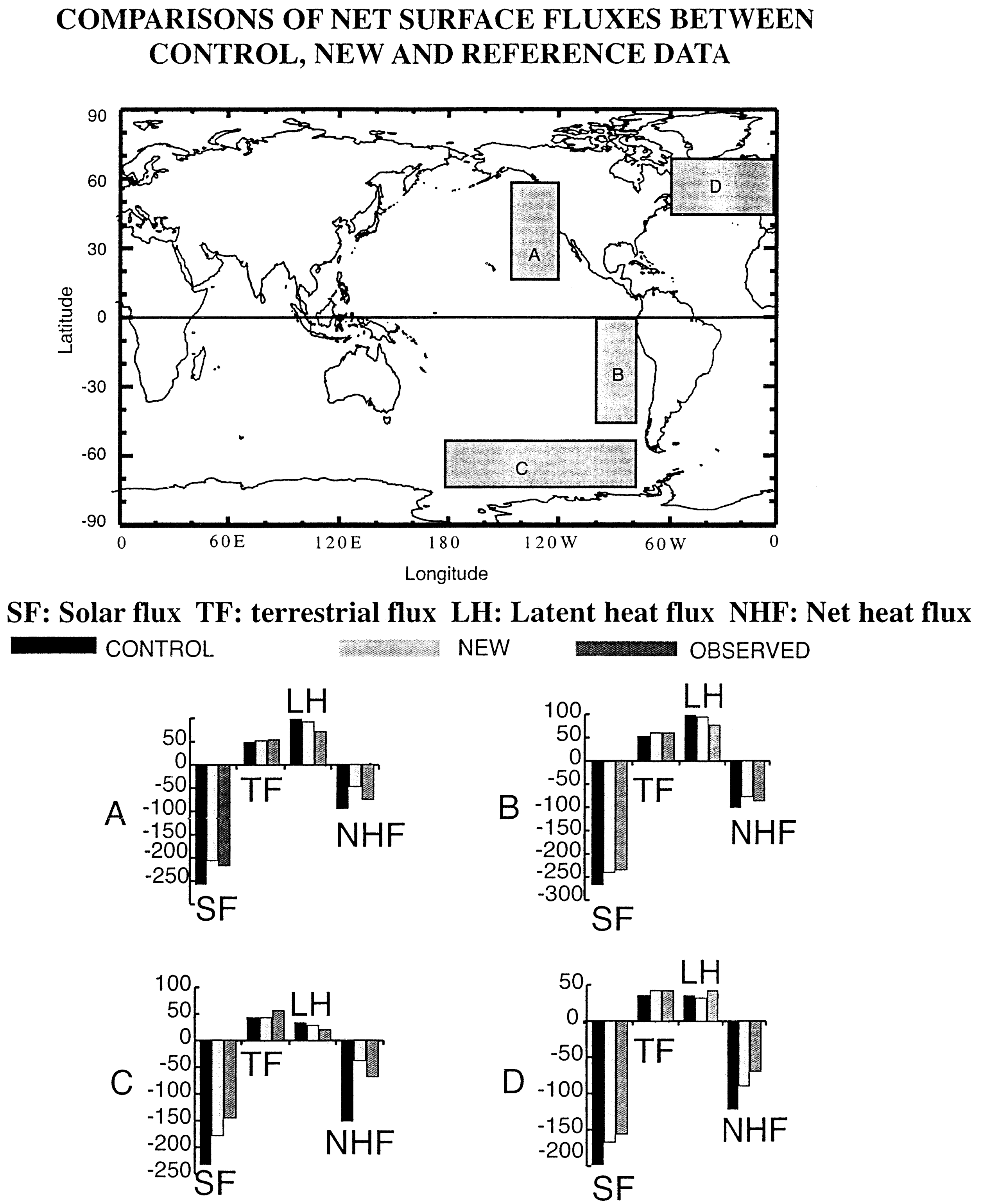

FIG. 6. Location of the four oceanic regions under investigation. Intercomparison of the monthly averaged (Jan, Jul, and Nov) simulated (with CONTROL and NEW versions) as well as observed net fluxes of latent (LH), solar (SF), terrestrial (TF), and net heat (NHF) fluxes at the surface (in W m^{-2}) in four regions: off the coast of California (region A; 20°–60°N, 120°–140°W) in Jul, off the coast of Peru (region B; 50°S–0°, 70°–100°W) in Nov, northern Atlantic Ocean (region C; 45°–75°N, 0°–60°W) in Jul, and Southern Hemispheric low pressure belt (region D; 50°–75°S, 80°–180°W) in Jan.

regions, model values of terrestrial, latent, and sensible (not shown) heat fluxes at the surface are not affected much by the revision and are close to the observed values. For the net solar fluxes at the surface, values with NEW can be up to 50 W m^{-2} lower than with CONTROL in regions A and C. Concerning regional averages, reductions amount to 52 W m^{-2} in A, 24 W m^{-2} in B, 53 W m^{-2} in C and 30 W m^{-2} in D. These reductions are due to increased regional cloud optical thickness rather than increased cloud pressure thickness.

4. Summary and discussion

Marine stratocumulus clouds are known to significantly affect the surface energy budget and act as important climate regulators because of their high albedo. In this study, we have demonstrated the sensitivity of AGCM simulations to the parameterization of the radiative properties of stratocumulus clouds in the model. An AGCM with prescribed SSTs can produce realistic simulations of stratocumulus cloud incidence even though their solar radiative properties are poorly represented. This is because the incidences of those clouds are basically determined by large-scale dynamics, near-surface moisture processes such as surface evaporation, and cloud-top entrainment rates, which are primarily influenced by the underlying SSTs. The liquid water path of stratocumulus clouds, on the other hand, is the most important parameter influencing the radiative characteristics of these clouds. We have presented a new formulation of stratocumlus cloud optical thickness based on consideration of the liquid water path. Our implementation of this formulation in the UCLA AGCM takes advantage of the unique PBL framework in the model. The liquid water path calculation in Eq. (3) is applicable to all GCMs with mixed layer PBLs.

Results from a 5-yr integration using an AGCM that incorporates this revision are very encouraging. We find that the revised model simulates a more realistic seasonal cycle of net surface heat and solar fluxes than the CONTROL version does. However, one has to recognize that the surface radiative fluxes estimated from satellite measurements are not observed directly. These fluxes are derived using retrieval schemes that have their own biases and deficiencies. Furthermore, the surface fluxes from the NCEP reanalysis data used in this study can only serve as a reference and should be considered as estimates.

We conclude that an AGCM, to be used in studies of the coupled atmosphere–ocean system, must not only realistically simulate the geographical distribution of stratocumulus clouds but also incorporate the effects of cloud physical properties needed for a correct estimation of radiative properties and surface fluxes.

Acknowledgments. The authors wish to thank Prof. A. Arakawa for his encouragement and useful comments. NCEP reanalysis data are provided by the NOAA–CIRES Climate Diagnostics Center, Boulder, Colorado, through their Web site (http://www.cdc.noaa.gov/). This research was funded under the following grants. NSF ATM-9613979, NASA NAG5-4420, DOE-CHAMMP-DE-FG03-96ER61214, and NOAA NA66GP0121. Model integrations were performed at the computer facilities of the UCLA Department of Atmospheric Sciences and the San Diego Supercomputer Center.

REFERENCES

Del Genio, A., M.-S. Yao, W. Kovari, and K. K.-W. Lo, 1996: A prognostic cloud water parameterization for global climate models. *J. Climate,* **9,** 270–304.

Gultepe, I., and G. A. Isaac, 1997: Liquid water content and temperature relationship from aircraft observations and its applicability to GCMs. *J. Climate,* **10,** 446–452.

Han, Q., W. B. Rossow, and A. A. Lacis, 1994: Near-global survey of effective droplet radii in liquid water clouds using ISCCP data. *J. Climate,* **7,** 465–497.

Harshvardhan, D. A. Randall, T. G. Corsetti, and D. A. Dazlich, 1989: Earth radiation budget and cloudiness simulations with a general circulation model. *J. Atmos. Sci.,* **46,** 1922–1942.

Klein, S. A., and D. L. Hartmann, 1993: The seasonal cycle of low stratiform clouds. *J. Climate,* **6,** 1587–1606.

Li, J.-L., and A. Arakawa, 1997: Improved simulation of the PBL moist processes with the UCLA GCM. Preprints, *Seventh Conf. on Climate Variation,* Long Beach, CA, Amer. Meteor. Soc., 35–40.

Li, Z., and H. G. Leighton, 1993: Global climatologies of solar radiation budgets at the surface and in the atmosphere from 5 years ERBE data. *J. Geophys. Res.,* **98,** 4919–4930.

Lilly, D. K., 1968: Models of cloud-topped mixed layers under a strong inversion. *Quart. J. Roy. Meteor. Soc.,* **94,** 292–309.

Ma, C.-C., C. R. Mechoso, A. W. Robertson, and A. Arakawa, 1996: Peruvian stratus clouds and the tropical Pacific circulation: A coupled ocean–atmosphere GCM study. *J. Climate,* **9,** 1635–1645.

Mechoso, C. R., J.-Y. Yu, and A. Arakawa, 2000: A coupled GCM pilgrimage: From climate catastrophe to ENSO simulations. *General Circulation Model Development: Past, Present and Future; Proceedings of a Symposium in Honor of Professor Akio Arakawa,* D. A. Randall, Ed., Academic Press, 539–575.

Neiburger, M., D. S. Johnson, and C.-W. Chien, 1961: *The Inversion over the Eastern North Pacific Ocean.* Vol. 1. *Studies of the Structure of the Atmosphere over the Eastern Pacific Ocean in Summer,* University of California Press, 94 pp.

Rossow, W. B., A. W. Walker, D. E. Beuschel, and M. D. Roiter, 1996: International Satellite Cloud Climatology Project (ISCCP) documentation of new cloud datasets. WMO/TD-No. 737, World Meteorological Organization, 115 pp.

Schubert, W. H., 1976: Experiments with Lilly's cloud-topped model. *J. Atmos. Sci.,* **33,** 436–446.

Stephens, G. L., 1978: Radiation profiles in extended water clouds. II. Parameterization schemes. *J. Atmos. Sci.,* **35,** 2123–2132.

Suarez, M. J., A. Arakawa, and D. A. Randall, 1983: The parameterization of the planetary boundary layer in the UCLA general circulation model: Formulation and results. *Mon. Wea. Rev.,* **111,** 2224–2243.

Sundqvist, H., 1978: A parameterization scheme for non-convective condensation including prediction of cloud water content. *Quart. J. Roy. Meteor. Soc.,* **104,** 677–690.

Wyngaard, J. C., and C.-H. Moeng, 1990: A global survey of PBL models used within GCMs. *Proceedings of a PBL Model Evaluation Workshop: European Centre for Medium-Range Forecasts,* P. Taylor and J. C. Wyngaard, Eds., World Climate Research Program Series 42, WMO/TD 378, 38–59.